Clinical Medicine & Research
Volume 2, Number 2: 99-106

http://www.mfldclin.edu/clinmedres

Original Research

Genotyping Parkinson Disease-Associated Mitochondrial Polymorphisms

Yiguo Jiang, PhD*, *National Farm Medicine Center, Marshfield Clinic Research Foundation, Marshfield, Wisconsin*
Tammy Ellis, BS, *National Farm Medicine Center, Marshfield Clinic Research Foundation, Marshfield, Wisconsin*
Anne R. Greenlee, PhD, *National Farm Medicine Center, Marshfield Clinic Research Foundation, Marshfield, Wisconsin*
** Current affiliation: Department of Biology, The University of New Mexico, Albuquerque, New Mexico*

ABSTRACT

OBJECTIVE

The purpose of this study was to establish a system for rapidly detecting single nucleotide polymorphisms (SNPs) in mitochondrial DNA (mtDNA) using hybridization probes and melting temperature (T_m) analysis. This technology should prove useful for population-based studies on the interaction between genetic factors and environmental exposures and the risk of Parkinson disease (PD).

METHODS

Mitochondrial DNA (mtDNA) was extracted from whole blood. Rapid polymerase chain reaction (PCR) and melting curve analyses were performed with primers and fluorochrome-labeled probes on a LightCycler (Roche Molecular Biochemical, Mannheim, Germany). Genotyping of 10 SNPs in 15 subjects was based on the analysis of allele-specific T_m of detection probes. The results of melting curve analyses were verified by sequencing all 150 PCR products.

RESULTS

Real-time monitoring showed optimal PCR amplification of each mtDNA fragment. The nucleotide changes at positions 1719, 4580, 7028, 8251, 9055, 10398, 12308, 13368, 13708, and 16391 from wild-type to mutant genotype resulted in 6.51, 8.29, 3.26, 7.82, 4.79, 2.84, 2.73, 9.04, 8.53, and 9.52°C declines in T_m of the detection probes, respectively. Genotyping of all 150 samples was verified by 100% correspondence with the results of sequencing. Fourteen subjects were haplogrouped by combining results for all 10 SNPs.

CONCLUSION

A rapid and reliable detection system for identifying mitochondrial polymorphisms and haplotypes was developed based on hybridization probe technology. This method may be suitable for mitochondrial genotyping of samples from large-scale epidemiology studies, and may prove useful for exploring the molecular etiopathogenesis of PD, identifying markers of genetic susceptibility, and protecting susceptible individuals from PD.

RECEIVED: **JANUARY 21, 2004**

REVISED AND ACCEPTED: **APRIL 20, 2004**

REPRINT REQUESTS:
Anne R. Greenlee, PhD
Marshfield Clinic Research Foundation
1000 North Oak Avenue
Mailstop: 2R5
Marshfield, WI 54449
Telephone: 715-389-4012
Fax: 715-389-3808
Email: greenlee.anne@mcrf.mfldclin.edu

KEYWORDS:
Parkinson disease; Mitochondrial DNA; DNA Polymorphism; DNA Hybridization; Genotype; Haplogroup

GRANT SUPPORT:
Funded by National Institute for Occupational Safety and Health (NIOSH grant 5U50 OH007543-02)

INTRODUCTION

Parkinson disease (PD) is one of the most prevalent neurodegenerative disorders, with approximately 1% of the population older than 65 years being affected.[1] The etiology of PD is still not fully understood, but genetic analyses, epidemiologic studies, and experimental models of PD are providing important new insights into the pathogenesis of PD.[2-6] In recent years, interest in interactions between genetic and environmental factors has spurred a number of association studies on polymorphisms of various genes.[7]

Growing evidence suggests that the interaction of environmental factors[8-10] and genetic predisposition may initiate the neurodegenerative process in PD.[11-13] One area of investigation has been the role of mitochondrial dysfunction in the pathogenesis of PD.[14,15] Studies suggest pesticides and other environmental toxins inhibiting complex I of the electron transport system may be involved in the pathogenesis of PD.[16] Indirect evidence suggests that, in some cases, the mitochondrial dysfunction in idiopathic PD may be due to mutations in mitochondrial DNA (mtDNA).[17-20] A single nucleotide polymorphism (SNP) leading to alterations in complex I activity may play a role in the pathogenesis of PD.[21] The activity of complex I is reduced within brains of patients with PD.[22] Whether enzyme deficiency is due to the presence of neurotoxins or to genetics, and how the interaction between environmental exposure and genetic factors influence the development of PD have not been established.

Restriction fragment length polymorphism (RFLP) studies of mtDNA from European Caucasoid, Native American, and African populations have revealed a number of stable polymorphic sites in mtDNA coding regions.[23-25] Related groups of polymorphic sites in mtDNAs are called haplogroups. Most mutations observed in mtDNA coding and control regions occur within these pre-existing haplogroups and define the individual mtDNA types or haplotypes. In comparison to individuals carrying the most common haplo-group, haplogroup H, individuals classified as haplogroup J and K demonstrate less risk of developing PD.[21] This protective effect is strongly associated with the SNP 10398G that defines haplogroups J and K. The absence of 10398G characterizes haplogroup U and may be associated with an increased risk of PD.[26] SNP 9055A may be associated with a protective effect for women.[21]

Population-based, case-control studies may assist with determining the interaction between host genetic factors (e.g., mitochondrial polymorphisms) and environmental exposures (e.g., pesticides, solvents and heavy metals) on the risk of PD.[27] Towards this goal, we developed a method to detect mtDNA polymorphisms that combines real-time polymerase chain reaction (PCR) with hybridization probes on the LightCycler (Roche Molecular Biochemical, Mannheim, Germany). The hybridization technology selected is based on the detection of two adjacent oligonucleotide probes, whose fluorescent labels communicate through fluorescence resonance energy transfer (FRET).[28,29] The anchor and sensor hybridization probes are added to the PCR and allowed to hybridize to an internal sequence of the PCR template. One probe is labeled at the 5′-end with the fluorophore LC Red 640, the other probe is labeled at the 3′-end with fluorescein. When these two probes hybridize to the PCR template, they are in close proximity, resulting in FRET between the two fluorophores. During FRET, the anchor fluorophore (fluorescein) is excited by the light source of the LightCycler instrument, and part of the excitation energy is transferred to the sensor fluorophore (LC Red 640). The LightCycler instrument monitors emitted fluorescence in real-time.

The fluorescence signal enables genotyping by analysis of the allele-specific melting behaviors of the sensor and anchor hybridization probes. The probe that is shorter has a lower melting temperature (T_m), spans the predicted polymorphism site and functions as a detection probe. During melting curve analysis, the temperature is slowly increased. If the sensor probe with a lower T_m is perfectly matched to its target sequence, it will melt away at a relatively high temperature. If this probe is mismatched, melting will occur at a lower temperature.[30,31] When the two dyes are no longer in close proximity, the fluorescence signal decreases.

Here, we report on a rapid detection system using hybridization probes to genotype 10 SNPs in the human mitochondrial genome to define mtDNA haplogroups. This methodology should assist with epidemiologic studies designed to gain a better understanding of populations at risk of PD.

MATERIALS AND METHODS

mtDNA extraction

The protocols used in this study were approved by the Marshfield Clinic Institutional Review Board. Whole blood samples in EDTA from 15 anonymous donors were provided by Marshfield Clinic Blood Bank within 24 hours of draw from a population that is ≥97% Caucasian.[32] The mtDNA was isolated from 100 µL of blood (mtDNA Extractor WB Kit, Wako Pure Chemical Industries, Ltd., Japan) and suspended in 10 mmol/L Tris (pH 7.4) containing 1 mmol/L EDTA. Any mtDNA not used immediately was stored at 4˚C for no longer than 7 days or frozen at –20˚C.

Design of primers and probes

Ten SNPs that define European mtDNA haplogroups located in sequences coding for genes and transcriptional control elements were chosen for genotyping according to the previous work of van der Walt et al. and Torroni et al.[21,23] Haplogroups were characterized by combining ten substitutions at nucleotide positions (np) 1719, 4580, 7028, 8251, 9055, 10398, 12308, 13368, 13708, and 16391. These nps were based on the revised Cambridge mitochondrial genomic sequence, Genbank accession number J01415.

Table 1 lists the sequences for PCR primers and hybridization probes used for SNP detection. Primers and probes were designed with LightCycler Probe Design software, version 1.0 (Roche Molecular Biochemical), except for the probes recognizing polymorphisms at np 10398 and 8251. The probes for these two nps were designed by TIB Molbiol LLC (Adelphia, NJ). Probes to detect SNPs at nps 1719, 4580, 8251, 9055, 10398, 13368, 13708, and 16391 were complementary to the antisense (reverse) strands of the mitochondrial genome, whereas probes to detect SNPs at nps 7028 and 12308 were complementary to the sense (forward) strands. A probe to detect the nucleotide at np 7028 corresponded to the mutation, while the other nine pairs of probes corresponded to the wild-type sequences.

Table 1. PCR primers, anchor, and sensor hybridization probes for SNP detection in mtDNA.

Target SNP	5′-3′ Sequence*	Position† (np)	Product Size (bp)
G1719A			
F. primer‡	GTAGCTTAACACAAAGCACC	1608-1801	194
R. primer	TCATCTTTCCCTTGCGG		
A. probe	GCCAGGTTTCAATTTCTATCGCCTATACTTTATT		
S. probe	GGTAAATGGTTTGG**C**TAAGGTTGT		
G4580A			
F. primer	ATACCCTTCCCGTACTAAT	4453-4660	208
R. primer	GCTTGCGTGAGGAAAT		
A. probe	GCTAG**C**ATGTTTATTTCTAGG		
S. probe	TACTCAGGTAAAAAATCAGTGCGAGCTTAGC		
C7028T			
F. primer	AATGATCTGCTGCAGTG	6901-7094	194
R. primer	AAATCAGTGAATGAAGCCT		
A. probe	CACTAGACATCGTACTACACGACACG		
S. probe	CTACGTTGTAGC**T**CACTTCCAC		
G8251A			
F. primer	CAAACCACTTTCACCGCT	8126-8371	246
R. primer	GGGCATTTCACTGTAAAGAG		
A. probe	GGGTAGAGGGGGTGCTATAGGGT		
S. probe	AATACGGGCC**C**TATTTCAAAG		
G9055A			
F. primer	TATCGAAACCATCAGCCT	8955-9147	193
R. primer	GGCGACAGCGATTTCT		
A. probe	TGATAAGTGTAGAGGGAAGGTTAATGGTTGAT		
S. probe	TGCTAGGGTGG**C**GCTT		
A10398G			
F. primer	CAAACAACTAACCTGCCAC	10296-10480	185
R. primer	ATGAGGGGCATTTGGTA		
A. probe	ACCAATTCGG**T**TCAGTCTAATCCT		
S. probe	TTGTAGTCACTCATAGGCCAGACTTAGGG		
A12308G			
F. primer	CACAAGAACTGCTAACTCA	12216-12403	188
R. primer	GGGTGGTAAGGATGGG		
A. probe	CATTGGTCTTAGGCCCCAA**A**AAT		
S. probe	TGGTGCAACTCCAAATAAAAGTAATAACCATGC		
G13368A			
F. primer	GTTACAATCGGCATCAACC	13279-13477	199
R. primer	CTAATGCTAGGCTGCCA		
A. probe	TGGA**C**CCGGAGCACATAAAT		
S. probe	TATGGCTTTGAAGAAGGCGTGGGT		
G13708A			
F. primer	CCTAACAGGTCAACCTCG	13626-13825	200
R. primer	CTAGGAAAGTGACAGCG		
A. probe	GTTAGTAATGAGAAATCCTGCGAATAGGCT		
S. probe	CGGCTG**C**CAGGCGTTTAA		
G16391A			
F. primer	AAGTCATTTACCGTACATAGC	16317-16509	193
R. primer	AGGAACCAGATGTCGGA		
A. probe	TTGATTTCACGGAGGATGGTGGT		
S. probe	AGGGA**C**CCCTATCTGAGGG		

* The position of base alteration in probes is underlined.

† Based on revised Cambridge mitochondrial genome (Genbank accession number J01415).

‡ F. primer, forward primer; R. primer, reverse primer; A. probe, anchor probe; S. probe, sensor probe.

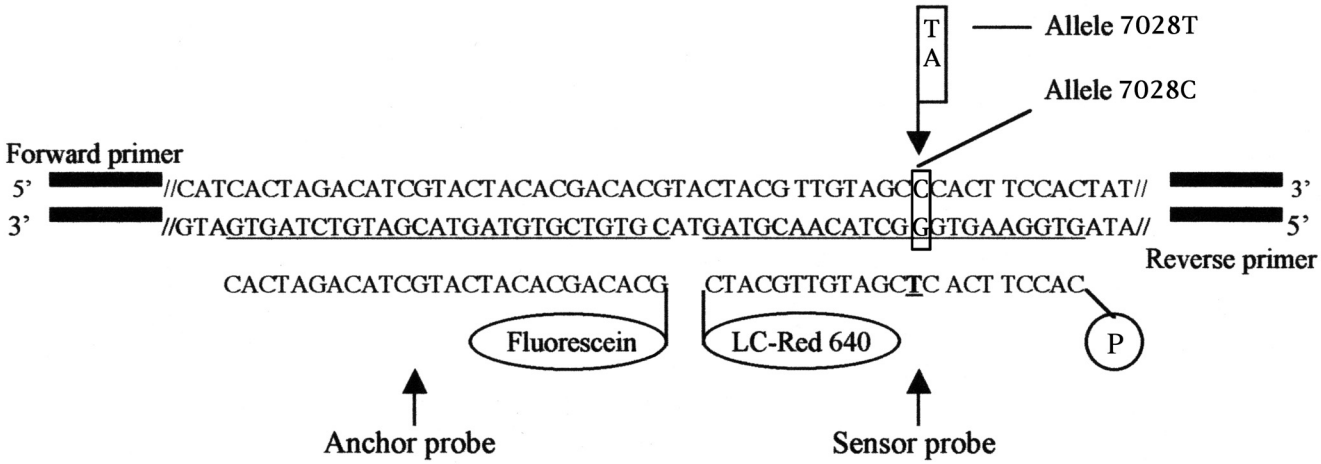

Figure 1. Orientation of mitochondrial DNA, PCR primers, amplicon, and the fluorophore-labeled hybridization probes for SNP C7028T. This probe corresponds to the mutation. The polymorphism at nucleotide 7028 is the result of a C to T substitution, which creates an A-T match between the antisense strand and the sensor probe. Complete matching of sensor probe to the antisense strand results in a higher T_m of the hybrid. The mismatch destabilizes the hybrid such that a decrease in the probe T_m occurs.

Sensor probes were labeled at the 5′-end with LC Red 640 and phosphorylated on the 3′-end to block extension. The anchor probe was labeled on the 3′-end with fluorescein and was designed to bind at a distance of two bases from the sensor probes. The primers and probes were synthesized and purified by TIB Molbiol LLC. Figure 1 describes the orientation of the mtDNA template to PCR primers, amplicon, and hybridization probes.

mtDNA template amplification and SNP detection

The analysis was carried out using a LightCycler instrument, a rapid thermal cycler with a microvolume fluorimeter. Amplification of the mtDNA template and SNP detection were performed in a reaction volume of 20 µL with 0.25 µM each primer, 0.2 µM anchor probe and 0.4 µM sensor probe, 8 ng of mtDNA, and 4 µL Master Mix from LightCycler FastStart DNA Master^{PLUS} Hybridization Probe Kit (Roche Applied Science, Penzberg, Germany). The mtDNA samples and reagents were pipetted into glass capillary cuvettes (Roche Diagnostics Corporation, Mannheim, Germany) and centrifuged to pool all components at the bottom of the capillary tube.

The LightCycler was programmed for pre-incubation at 95˚C for 10 minutes (to activate FastStart Polymerase), amplification of target mtDNA (28-47 cycles of denaturation at 95˚C for 10 seconds, annealing at 55˚C for 10 seconds, and extension at 72˚C for 10 seconds), melting curve analysis, and cooling of the sample carousel. LC Red 640 was monitored on channel 2 (F2). The number of amplification cycles was 28 for SNP 10398; 29 for SNP 16391; 30 for SNPs 1719, 7028, 12308, and 13368; 31 for SNP 9055; 32 for SNP 4580; 34 for SNP 13708; and 47 for SNP 8251. The temperature transition rates were programmed at 20˚C/second. Fluorescence was measured in a single step at the end of the annealing period of each cycle to monitor amplification. The number of amplification cycles was varied to ensure that each amplification curve would begin a "hook effect," which is defined as an exponential rise of the fluorescence signal followed by a drop in later cycles. Total run time ranged between 60 and 90 minutes and varied with the optimal number of amplification and melting cycles.

Melting analysis was performed following template amplification. Fluorescence was measured continuously during the slow temperature rise to monitor the dissociation of the shorter probe from the amplicon. The melting curve was initiated by cooling the reaction mixture to 45˚C at 20˚C/second, holding it at 45˚C for 45 seconds, and then slowly heating it to 80˚C at 0.1˚C/second. Multiple melting cycles were conducted with the same amplified product to optimize the melting curve shape and to better discriminate between allele-specific T_m. One melting cycle was performed for SNP 1719; 2 cycles for SNP 8251; 4 cycles for SNPs 10398, 12308, and 13368; 5 cycles for SNP 9055; 6 cycles for SNPs 7028 and 16391; and 7 cycles for SNPs 4580 and 13708. Samples were held at 4˚C upon completion of cycling. Fluorescence (F2) was plotted against temperature (T) to produce melting curves for each sample. Melting curves were then converted to melting peaks by plotting the negative derivative of the fluorescence with respect to temperature against temperature (–d(F2)/dT versus T) using version 3.5 of the LightCycler® software.

Sequencing

Results of genotyping with hybridization probes were compared to PCR amplicon sequences to verify melting curve analyses. PCR products were purified using the QIAquick PCR purification kit (QIAGEN Inc., Valencia, CA). Purified PCR products were then sequenced using BigDye Terminator V3.1 Cycle Sequencing Kit (Applied Biosystems, Foster City, CA). The sequencing reaction contained 1.5 µL (1.5 ng) of purified PCR product, 4 µL of BigDye Cycle Sequencing Mix, 1.28 µL of primer (1.6 pmol), and 3.22 µL H_2O. Thermal cycling conditions were

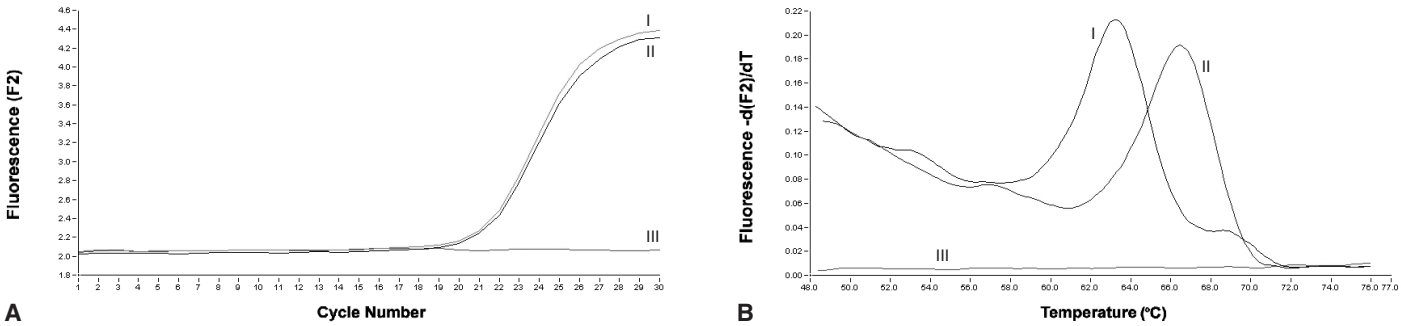

Figure 2. PCR amplification and genotyping of C7028T SNP using hybridization probes and melting curve analysis. **(A)** Plot of fluorescence intensity signal (F2) versus cycle number for SNP 7028. The 194 bp fragment which covers the 7028 site was amplified from genomic mtDNA of two different genotypes, either 7028C allele (curve I) or 7028T allele (curve II). The no-template control (curve III) shows no amplification. **(B)** Following amplification a melting analysis of amplified fragments was immediately performed. Data for the plot was obtained during the melting transition of the probe from the amplified fragment. The melting curves were plotted for a sample for the 7028C allele (curve I) and a sample for the 7028T allele (curve II). Melting analysis of a no-template control (curve III) was also performed. The melting peaks indicate that the 7028C allele sequence has a lower T_m than the 7028T allele sequence due to homology between the probe and mutant allele.

25 cycles of 96˚C for 10 seconds, 50˚C for 5 seconds, and 60˚C for 4 minutes. Unincorporated primers and dye terminators were removed using DyeEx 96 plates (QIAGEN GmbH, Hilden, Germany). Purified samples were dried at 70˚C and rehydrated with 10 µL of Hi-Di™ Formamide (Applied Biosystems). Samples were denatured at 95˚C for 2 minutes and immediately chilled on ice for 2 minutes. Sequencing was performed on an ABI PRISM 3100 Genetic Analyzer (Applied Biosystems) with 3100 Genetic Analyzer Data Collection software, version 1.1. Sequencing analysis was performed using Lasergene SeqMan II software (DNASTAR, Inc., Madison, WI). Amplicon sequences were aligned with the revised Cambridge mtDNA genome sequence using BLAST 2 SEQUENCES software (http://www.ncbi.nlm.nih.gov/blast/bl2seq/bl2.html) to locate and identify base changes.

RESULTS

We extracted 1.1 ± 0.7 µg mtDNA from 100 µL whole blood samples (n=15) in approximately 1.5 hours. The mtDNA purity and concentration were adequate for PCR amplification and unambiguous SNP detection. A total of 150 genotypes were evaluated encompassing 10 SNPs in mtDNA from 15 patient samples. Figure 2 provides an example of genotyping with primers and probes for variant C7028T. In contrast to the negative control (no template, curve III), PCR products for both alleles accumulated exponentially indicating PCR conditions were optimized (figure 2A, curves I and II). Hybridization of the detection probe to the target sequence was monitored by analysis of the melting curve. By plotting the fluorescence signal against the T_m it was possible to separate peak T_m for wild-type (7028C) and mutant alleles (7028T) (figure 2B). The peak T_m for 7028T was 66.37˚C (curve II), whereas the peak T_m for 7028C was 63.11˚C (curve I). The T_m for the 10 mtDNA wild-type and mutant alleles are provided in table 2. The T_m for wild-type alleles ranged between 55.61˚C and 65.66˚C, whereas the T_m for mutant alleles ranged between 49.32˚C and 66.37˚C. Variations from wild-type to mutant alleles resulted in T_m changes between 2.73˚C and 9.52˚C.

To verify results of melting curve analyses using hybridization probes, a total of 150 PCR products were sequenced and aligned with the complete human mitochondrial genome sequence. Amplicons were of the expected sizes and shared ≥99% homology with mitochondrial genome sequence (100% identity for wild-type samples, ≥99% identity for mutant samples).

Table 2. Observed T_m of wild-type (*wt*) and mutant (*mut*) alleles as determined by hybridization probes and LightCycler technology.

Allele (*wt/mut*)	Wild-type n*	Wild-type T_m (˚C) Mean ± S.D.	Mutant n†	Mutant T_m (˚C) Mean ± S.D.	ΔT_m (˚C) ($\lvert T_m$ *wt* – T_m*mut* $\rvert$)
G1719A	14	63.69 ± 0.04	3[a]	57.18 ± 0.06	6.51
G4580A	14	57.61 ± 0.18	3[a]	49.32 ± 0.05	8.29
C7028T	5	63.11 ± 0.10	10[d]	66.37 ± 0.09	3.26
G8251A	13	59.78 ± 0.08	3[b]	51.96 ± 0.07	7.82
G9055A	13	55.61 ± 0.18	3[b]	50.82 ± 0.04	4.79
A10398G	12	63.21 ± 0.08	3[c]	60.37 ± 0.06	2.84
A12308G	12	61.39 ± 0.05	3[c]	58.66 ± 0.04	2.73
G13368A	14	60.76 ± 0.08	3[a]	51.72 ± 0.05	9.04
G13708A	14	65.66 ± 0.15	3[a]	57.13 ± 0.13	8.53
G16391A	14	59.39 ± 0.05	3[a]	49.87 ± 0.04	9.52

* Numbers of samples, each analyzed once.
† Total number of detections (number of samples: a=1; b=2; c=3; d=10).

Single base changes at the targeted SNP sites corresponded with results of melting curve analyses. As shown in table 3, haplogroups of 14 out of 15 (93.3%) samples were identified by combining the patterns of SNPs according to previous definitions.[21,23] One sample could not be classified based on criteria for European haplogroups.

DISCUSSION

The LightCycler instrument and hybridization probe technology proved to be a powerful detection format for accurately and quickly genotyping SNPs by melting curve analysis. This protocol was capable of genotyping 32 samples in 60 to 90 minutes without enzyme digestion or electrophoresis. The method was performed in a closed system, eliminating potential problems with sample tracking and end product contamination. Accuracy and reliability of the fluorescence genotyping was demonstrated by >99% homology between the 150 genotypes and the published sequence for human mtDNA.

We were able to classify 14 of 15 mtDNA samples into 8 of 9 haplogroups based on SNP combinations encompassing Finnish, Swedish, Tuscan and European mtDNA populations.[21,23] Included in our study population were mtDNA haplogroups H, J, K, T, U, V, W and X. Haplogroup I was not identified in our samples which differed from the two previously cited studies. Haplogroup H, found most commonly in Scandinavian and European populations, represented 5 of 15 (33%) of our mtDNA study samples. Haplogroups K and W each were identified in 13% of our study samples. The haplogroups J, T, X, V, and U were each identified at a frequency of 7% in our study samples. One mtDNA sample (6%) was beyond the definition of haplogroups associated with European ancestry. This is consistent with two previous studies in which 2.4% of Caucasian samples[23] and 8.4% of Caucasian samples[21] were beyond these defined haplogroups.

Genotyping of SNPs by using fluorescent probes offers several advantages in comparison to the more common methodologies of RFLP analysis and DNA sequencing.[23-25,33,21] RFLP analysis relies on amplification of template, digestion of amplicon DNA with restriction enzymes, and subsequent sizing of the fragments by agarose gel electrophoresis. This approach is time consuming, labor intensive, and dependent on the presence of an appropriate restriction site and complete digestion, which cannot always be achieved. Some researchers employ only sequencing to detect mitochondrial mutations.[34,35] However, it is difficult to apply sequencing to large sample sizes because of cost and complexities of sample preparation.

Another platform for fluorescent probe chemistry and genotyping SNPs is the TaqMan Allelic Discrimination Assay. TaqMan has shown promise for large-scale genotyping of mtDNA polymorphisms when combined with DNA extraction systems and multi-well plates.[21] The assay uses the 5′ nuclease activity of *Taq* polymerase to generate a fluorescent reporter signal during PCR extension. For SNP genotyping, one pair of TaqMan probes and one pair of PCR primers are used. The assay uses two TaqMan probes that differ at the polymorphic site, with one probe complementary to the wild-type allele and the other to the variant allele. Reporter and quencher dyes are covalently linked to the 5′ and 3′ ends of the wild-type and variant probes. When the probes are intact, fluorescence is quenched because of the physical proximity of the reporter and quencher dyes. During the PCR annealing step, the TaqMan probes hybridize to either the wild-type or polymorphic site. During the PCR extension phase, the 5′ reporter dye is cleaved by the 5′ nuclease activity of the *Taq* polymerase, leading to an increase in fluorescence of the reporter dye. Specific genotyping is determined by measuring the signal intensity of the reporter dye after the PCR reaction.[36] Limitations of this approach include difficulties designing specific probes without knowing the

Table 3. Results of genotyping and haplogroup definitions.

		SNP*									
Sample Number	Haplo-group	G1719A	G4580A	C7028T	G8251A	G9055A	A10398G	A12308G	G13368A	G13708A	G16391A
1	H	G	G	C	G	G	A	A	G	G	G
2	W	G	G	T	A	G	A	A	G	G	G
3	U	G	G	T	G	G	A	G	G	G	G
4	T	G	G	T	G	G	A	A	A	G	G
5	Other	G	G	T	G	G	A	A	G	G	A
6	K	G	G	T	G	A	G	G	G	G	G
7	J	G	G	T	G	G	G	A	G	A	G
8	K	G	G	T	G	A	G	G	G	G	G
9	W	G	G	T	A	G	A	A	G	G	G
10	X	A	G	T	G	G	A	A	G	G	G
11	H	G	G	C	G	G	A	A	G	G	G
12	H	G	G	C	G	G	A	A	G	G	G
13	V	G	A	T	G	G	A	A	G	G	G
14	H	G	G	C	G	G	A	A	G	G	G
15	H	G	G	C	G	G	A	A	G	G	G

* SNPs are numbered from the first nucleotide of complete mitochondrial genome (Genbank accession number J01415).

sequence of all possible allelic variants, background fluorescence due to nonspecific binding between probes and target sequences, and an inability to measure the size of amplicons. Negative reactions may require sequencing for verification.

LightCycler technology minimizes these difficulties by monitoring shifts in melting temperatures of hybrids comprised of probe and wild-type or variant alleles. Fluorescence due to FRET occurs only when both probes anneal to the target sequence, reducing nonspecific background signals. Amplicon size is predicted by its direct relationship to T_m. Individual or multiple base changes due to insertions, deletions, and substitutions can be detected simultaneously. The principal drawback is the size of the carousel, which limits the number of samples to 32 per run.

Single base mismatches may lower the T_m of hybridization probes by several degrees Celsius.[37] The amount of destabilization depends on the specific mismatch, neighboring nucleotides, and the position of the mutation within the sequence of the probe.[38] Minor differences in T_m (<1˚C) can be distinguished because of the reproducibility of the nucleic acid T_m. We achieved differences in T_m ranging between 2.73˚C and 9.52˚C, suggesting our anchor and sensor probes were properly designed for screening single nucleotide variations. Our standard deviations were <0.2˚C, consistent with previously reported values.[39]

Typically, total DNA fractions are used to analyze mtDNA, although mtDNA occupies only a small portion of nucleic acid isolates.[21,40] Isolation of mtDNA using the mtDNA Extractor WB Kit is efficient and enables simultaneous preparation of mtDNA from multiple samples for screening assays. We extracted approximately 1 µg mtDNA from 100 µL blood samples. Robust amplification of mtDNA sequences was achieved using nanogram quantities of template and real-time PCR. Nonspecific amplification of genomic DNA sequences was minimized using template preparations enriched with mtDNA.

Hybridization probe technology and melting curve analysis may have clinical, as well as research applications.[39] The procedure has been multiplexed for the simultaneous detection of five polymorphisms modifying drug sensitivity and for SNPs in human cytochrome P450 enzymes involved in drug metabolism.[41,42] Optimizing conditions for 10 different SNPs required changing the number of amplification or melting cycles without modifying reagent source or concentration. Necessary modifications were identified in real-time without setting up *de novo* reactions.

In summary, we have developed an assay system for rapidly genotyping and haplogrouping mitochondrial polymorphisms based on hybridization probe technology and melting curve analysis. Genotyping of 10 SNPs in 32 samples was accomplished in approximately 1 to 1.5 hours, making this method well suited for typing a variety of mitochondrial polymorphisms for association studies.

ACKNOWLEDGMENTS

The authors thank Jeffery M. Vance, MD, PhD and William K. Scott, PhD for suggesting we pursue mitochondrial haplogrouping for our association study; Joelle van der Walt, PhD for providing assistance with verifying mtDNA SNP sites; James K. Burmester, PhD for reviewing this manuscript; Patricia Kucinski, PhD for her assistance with designing probes for SNPs 10398 and 8251; Alice Stargardt and Linda Weis for editorial assistance; and Tom Brunette in graphic arts for assistance with the preparation of figures.

REFERENCES

1. Adams RD, Victor M. Part 4/The major categories of neurologic disease. In: Principles of Neurology. 5th ed. New York, NY: McGraw-Hill; 2001. 1128-1138.
2. Siderowf A, Stern M. Update on Parkinson disease. Ann Intern Med 2003;138:651-658.
3. Dawson TM, Dawson VL. Rare genetic mutations shed light on the pathogenesis of Parkinson disease. J Clin Invest 2003;111:145-151.
4. Betarbet R, Sherer TB, Greenamyre JT. Animal models of Parkinson's disease. Bioessays 2002;24:308-318.
5. Warner TT, Schapira AH. Genetic and environmental factors in the cause of Parkinson's disease. Ann Neurol 2003;53 (suppl 3):S16-S23.
6. Beal MF. Experimental models of Parkinson's disease. Nat Rev Neurosci 2001;2:325-334.
7. Tan EK, Khajavi M, Thornby JI, Nagamitsu S, Jankovic J, Ashizawa T. Variability and validity of polymorphism association studies in Parkinson's disease. Neurology 2000;55:533-538.
8. Priyadarshi A, Khuder SA, Schaub EA, Shrivastava S. A meta-analysis of Parkinson's disease and exposure to pesticides. Neurotoxicology 2000;21:435-440.
9. Priyadarshi A, Khuder SA, Schaub EA, Priyadarshi SS. Environmental risk factors and Parkinson's disease: a metaanalysis. Environ Res 2001;86:122-127.
10. Pezzoli G, Canesi M, Antonini A, Righini A, Perbellini L, Barichella M, Mariani CB, Tenconi F, Tesei S, Zecchinelli A, Leenders KL. Hydrocarbon exposure and Parkinson's disease. Neurology 2000;55:667-673.
11. Payami H, Larsen K, Bernard S, Nutt J. Increased risk of Parkinson's disease in parents and siblings of patients. Ann Neurol 1994;36:659-661.
12. Mizuno Y, Ikebe S, Hattori N, Nakagawa-Hattori Y, Mochizuki H, Tanaka M, Ozawa T. Role of mitochondria in the etiology and pathogenesis of Parkinson's disease. Biochim Biophys Acta 1995;1271:265-274.
13. Ben-Shlomo Y, Sieradzan K. Idiopathic Parkinson's disease: epidemiology, diagnosis and management. Br J Gen Pract 1995;45:261-268.
14. Gu M, Cooper JM, Taanman JW, Schapira AH. Mitochondrial DNA transmission of the mitochondrial defect in Parkinson's disease. Ann Neurol 1998;44:177-186.
15. Brown MD, Shoffner JM, Kim YL, Jun AS, Graham BH, Cabell MF, Gurley DS, Wallace DC. Mitochondrial DNA sequence analysis of four Alzheimer's and Parkinson's disease patients. Am J Med Genet 1996;61:283-289.
16. Sherer TB, Betarbet R, Greenamyre JT. Environment, mitochondria, and Parkinson's disease. Neuroscientist 2002;8:192-197.

17. Simon DK, Pulst SM, Sutton JP, Browne SE, Beal MF, Johns DR. Familial multisystem degeneration with parkinsonism associated with the 11778 mitochondrial DNA mutation. Neurology 1999;53:1787-1793.
18. Calabrese V, Scapagnini G, Giuffrida Stella AM, Bates TE, Clark JB. Mitochondrial involvement in brain function and dysfunction: relevance to aging, neurodegenerative disorders and longevity. Neurochem Res 2001;26:739-764.
19. Vives-Bauza C, Andreu AL, Manfredi G, Beal MF, Janetzky B, Gruenewald TH, Lin MT. Sequence analysis of the entire mitochondrial genome in Parkinson's disease. Biochem Biophys Res Commun 2002;290:1593-1601.
20. Dawson TM, Dawson VL. Molecular pathways of neurodegeneration in Parkinson's disease. Science 2003;302:819-822.
21. van der Walt JM, Nicodemus KK, Martin ER, Scott WK, Nance MA, Watts RL, Hubble JP, Haines JL, Koller WC, Lyons K, Pahwa R, Stern MB, Colcher A, Hiner BC, Jankovic J, Ondo WG, Allen FH Jr, Goetz CG, Small GW, Mastaglia F, Stajich JM, McLaurin AC, Middleton LT, Scott BL, Schmechel DE, Pericak-Vance MA, Vance JM. Mitochondrial polymorphisms significantly reduce the risk of Parkinson disease. Am J Hum Genet 2003;72:804-811.
22. Schapira AH, Cooper JM, Dexter D, Clark JB, Jenner P, Marsden CD. Mitochondrial complex I deficiency in Parkinson's disease. J Neurochem 1990;54:823-827.
23. Torroni A, Huoponen K, Francalacci P, Petrozzi M, Morelli L, Scozzari R, Obinu D, Savontaus ML, Wallace DC. Classification of European mtDNAs from an analysis of three European populations. Genetics 1996;144:1835-1850.
24. Torroni A, Schurr TG, Cabell MF, Brown MD, Neel JV, Larsen M, Smith DG, Vullo CM, Wallace DC. Asian affinities and continental radiation of the four founding Native American mtDNAs. Am J Hum Genet 1993;53:563-590.
25. Graven L, Passarino G, Semino O, Boursot P, Santachiara-Benerecetti S, Langaney A, Excoffier L. Evolutionary correlation between control region sequence and restriction polymorphisms in the mitochondrial genome of a large Senegalese Mandenka sample. Mol Biol Evol 1995;12:334-345.
26. van Der Walt JM, Nicodemus KK, Martin ER, Scott WK, Nance MA, Hubble JP, Haines JL, Koller WC, Pahwa R, Stern M, Hiner BC, Jankovic J, Goetz CG, Small GW, Mastaglia F, Gibson RA, Middleton LT, McLaurin AC, Pericak-Vance MA, Vance JM. Specific mitochondrial haplogroups affect risk for late-onset Parkinson disease. Am J Hum Genetics 2002;71(suppl):364(abstract).
27. Greenlee AR, Burmester JK, Hiner BC. Pesticide exposure, host susceptibility factors and risk of Parkinson's disease: an introduction to a work in progress. WMJ 2002;101:20-24.
28. Wittwer CT, Ririe KM, Andrew RV, David DA, Gundry RA, Balis UJ. The LightCycler: a microvolume multisample fluorimeter with rapid temperature control. Biotechniques 1997;22:176-181.
29. Lyon E. Mutation detection using fluorescent hybridization probes and melting curve analysis. Expert Rev Mol Diagn 2001;1:92-101.
30. Torres MJ, Criado A, Palomares JC, Aznar J. Use of real-time PCR and fluorimetry for rapid detection of rifampin and isoniazid resistance-associated mutations in *Mycobacterium* tuberculosis. J Clin Microbiol 2000;38:3194-3199.
31. Gatke MR, Viby-Mogensen J, Bundgaard JR. Rapid simultaneous genotyping of the frequent butyrylcholinesterase variants Asp70Gly and Ala539Thr with fluorescent hybridization probes. Scand J Clin Lab Invest 2002;62:375-383.
32. Greenlee RT. Measuring disease frequency in the Marshfield epidemiologic study area (MESA). Clin Med Res 2003;1:273-280.
33. Tan EK, Chai A, Zhao Y, Lum SY, Fook-Chong SM, Teoh ML, Yih Y, Pavanni R, Wong MC. Mitochondrial complex I polymorphism and cigarette smoking in Parkinson's disease. Neurology 2002;59:1288-1289.
34. Kirchner SC, Hallagan SE, Farin FM, Dilley J, Costa-Mallen P, Smith-Weller T, Franklin GM, Swanson PD, Checkoway H. Mitochondrial ND1 sequence analysis and association of the T4216C mutation with Parkinson's disease. Neurotoxicology 2000;21:441-445.
35. Herrnstadt C, Elson JL, Fahy E, Preston G, Turnbull DM, Anderson C, Ghosh SS, Olefsky JM, Beal MF, Davis RE, Howell N. Reduced-median-network analysis of complete mitochondrial DNA coding-region sequences for the major African, Asian, and European haplogroups. Am J Hum Genet 2002;70:1152-1171.
36. von Ahsen N, Oellerich M, Schutz E. DNA base bulge vs unmatched end formation in probe-based diagnostic insertion/deletion genotyping: genotyping the UGT1A1 (TA)(n) polymorphism by real-time fluorescence PCR. Clin Chem 2000;46:1939-1945.
37. Wetmur JG. DNA probes: applications of the principles of nucleic acid hybridization. Crit Rev Biochem Mol Biol 1991;26:227-259.
38. Nauck M, Wieland H, Marz W. Rapid, homogeneous genotyping of the 4G/5G polymorphism in the promoter region of the PAII gene by fluorescence resonance energy transfer and probe melting curves. Clin Chem 1999;45:1141-1147.
39. Lyon E, Millson A, Phan T, Wittwer CT. Detection and identification of base alterations within the region of factor V Leiden by fluorescent melting curves. Mol Diagn 1998;3:203-209.
40. Shi MM. Enabling large-scale pharmacogenetic studies by high-throughput mutation detection and genotyping technologies. Clin Chem 2001;47:164-172.
41. Hiratsuka M, Narahara K, Kishikawa Y, Ismail Hamdy S, Endo N, Agatsuma Y, Matsuura M, Inoue T, Tomioka Y, Mizugaki M. A simultaneous LightCycler detection assay for five genetic polymorphisms influencing drug sensitivity. Clin Biochem 2002;35:35-40.
42. Stamer UM, Bayerer B, Wolf S, Hoeft A, Stuber F. Rapid and reliable method for cytochrome P450 2D6 genotyping. Clin Chem 2002;48:1412-1417.